Mecánica Computacional Vol. XXIII, pp. 2907-2922
G.Buscaglia, E.Dari, O.Zamonsky (Eds.)
Bariloche, Argentina, November 2004

THE KLE METHOD: A VELOCITY-VORTICITY FORMULATION FOR THE NAVIER-STOKES EQUATIONS

Fernando L. Ponta[*†]

[*]College of Engineering
University of Buenos Aires
Av. Paseo Colón 850, Buenos Aires, 1063, Argentina
e-mail: fponta@fi.uba.ar

[†]Department of Theoretical and Applied Mechanics
University of Illinois at Urbana-Champaign
104 S. Wright St., Urbana, IL 61801, USA
e-mail: ponta@uiuc.edu

Key Words: vorticity-velocity formulation, Navier-Stokes equations, time-space split algorithm, finite element method.

Abstract. *In this work, a novel procedure for the Navier-Stokes equations in the vorticity-velocity formulation is presented. The time evolution of the vorticity is solved as an ODE problem on each node of the spatial discretization, using at each step of the time discretization the spatial solution for the velocity field provided by a new PDE expression called the kinematic Laplacian equation (KLE). This complete decoupling of the two variables in a vorticity-in-time/velocity-in-space split algorithm reduces the number of unknowns to solve in the time-integration process and also favors the use of advanced ODE algorithms enhancing the efficiency and robustness of time integration. The issue of the imposition of vorticity boundary conditions is addressed, as well as the details of the implementation of the KLE by isoparametric finite element discretization. We shall see some validation results of the KLE method applied to the classical case of a circular cylinder in impulsive-started pure-translational steady motion at several Reynolds numbers in the range* $5 < Re < 180$*, comparing them with experimental measurements and flow visualization plates; and finally, a recent result from a study on periodic vortex-array structures produced in the wake of forced-oscillating cylinders.*

1 INTRODUCTION

During the last three decades several studies appeared concerning the representation of the Navier–Stokes equations in terms of nonprimitive variables (namely the vorticity and the velocity potentials) instead of the classical formulation in terms of the primitive variables velocity and pressure. This family of approaches is generally known as vorticity-stream function ($\boldsymbol{\omega}$, $\boldsymbol{\psi}$) methods. More recently, together with those works on the vorticity-stream function formulation and as a natural extension of them, a comparatively smaller number of studies were presented using a hybrid formulation in terms of the primitive and nonprimitive variables velocity and vorticity. As several authors pointed out,[1–3] the vorticity-velocity ($\boldsymbol{\omega}$, $\boldsymbol{v}$) methods (as they are generally known) present some advantages compared with the classical formulation on primitive variables or with the vorticity-stream function methods, namely: a) The pair of variables involved is particularly suited for a dynamic description of incompressible viscous flows. The vorticity is governed by a well understood dynamical equation while the velocity, which embodies the kinematical aspect of the problem, can be related to the vorticity by a simple elliptic equation. In vortex-dominated flows the vorticity advection is a fundamental process determining the dynamics of the flow, hence the vorticity-velocity description is closer to physical reality. b) The variety of boundary conditions that can be chosen for the velocity potentials due to the nonuniqueness of the velocity representation is avoided since the velocity is supplemented by unique boundary conditions. c) In some specific situations like that of external flows, boundary conditions at infinity are easier to implement for the vorticity than for the pressure. d) The noninertial effects only enter the solution procedure of the ($\boldsymbol{\omega}$, $\boldsymbol{v}$) formulation via the proper implementation of the initial and boundary conditions. Hence, the general applicability of an algorithm based on the ($\boldsymbol{\omega}$, $\boldsymbol{v}$) formulation is enhanced because it is independent of whether or not the frame of reference is inertial.

The first uses of the ($\boldsymbol{\omega}$, $\boldsymbol{v}$) formulation of the incompressible Navier–Stokes equations were reported by Fasel[4] who analyzed the stability of boundary layers in two dimensions and by Dennis, Ingham and Cook[5] who derived a numerical method for computing steady-state three-dimensional flows. Both approach were based on finite difference techniques. Since then several investigations have been conducted on incompressible hybrid variable models using variations of the finite difference approach (e.g. see,[6–8] among others). A vorticity-velocity finite element solution of the three-dimensional compressible Navier–Stokes equations have been presented by Guevremont *et al.*[9] who investigated the steady state flow in a cubic cavity for several Mach numbers. More recently Clerxc,[2] then Davies and Carpenter,[10] introduced pseudospectral procedures for the ($\boldsymbol{\omega}$, $\boldsymbol{v}$) formulation. Lo and Young[11] presented an arbitrary Lagrangian-Eulerian ($\boldsymbol{\omega}$, $\boldsymbol{v}$) method for two-dimensional free surface flow, using finite difference discretization for the free surface and finite element discretization for the interior of the domain.

A disadvantage of the vorticity-velocity formulation, compared with the formulation

in primitive variables is that in the most general three-dimensional case the ($\boldsymbol{\omega}$, $\boldsymbol{v}$) formulation requires a total of six equations to be solved instead of the usual four of the primitive-variable approach.[2] The objective of the present study is to introduce a new method based on the ($\boldsymbol{\omega}$, $\boldsymbol{v}$) formulation which aims to tackle this six-unknown question and to improve some other aspects of the numerical implementation of the ($\boldsymbol{\omega}$, $\boldsymbol{v}$) approach. This alternative method is characterized by a complete decoupling of the two variables in a vorticity-in-time/velocity-in-space split algorithm, thus reducing to three the number of unknowns to solve in the time integration process. As we shall see later on, this time-space splitting also favors the use of adaptive variable-stepsize/variable-order ODE algorithms which enhances the efficiency and robustness of the time integration process.

A comprehensive study of the theoretical basis of the vorticity-velocity formulation in two and three dimensions can be found in chapter 4 of Quartapelle,[1] including a series of theorems proving the equivalence between the ($\boldsymbol{\omega}$, $\boldsymbol{v}$) formulation of the incompressible Navier–Stokes equations and their classical formulation in primitive variables (velocity-pressure).

1.1 Vorticity boundary conditions

A common problem to all the methods based on nonprimitive or hybrid variables is the absence of boundary conditions for the vorticity in presence of no-slip boundary conditions for the velocity. In the case of the ($\boldsymbol{\omega}$, $\boldsymbol{\psi}$) formulation it also implies that the Poisson problem for the stream function with both Dirichlet and Neumann conditions is overdetermined. There are several different ways of overcoming this difficulty. Some earlier approaches like the *boundary vorticity formula* or the *vorticity creation* methods use different techniques to define the boundary values of vorticity in terms of the stream function (or the velocity) by means of some approximate formula applied locally at the no-slip boundary. They are roughly equivalent, however their implementation may differ remarkably depending on the type of discretization used (see[1, 12–14]).

An alternative viewpoint have been introduced by Quartapelle and Valz-Gris.[15, 16] They showed that in order to satisfy the no-slip boundary conditions for the velocity, the vorticity should be subject to an integral constraint. This integral condition enforces the orthogonality of the abstract projection of the vorticity field with respect to the linear space of the harmonic functions defined on the domain. This condition is a direct consequence of the boundary conditions on the velocity, and ensure satisfaction of essential conservation laws for the vorticity. An important aspect of the integral vorticity conditions is their nonlocal character: the vorticity distribution in the interior of the domain and on its boundary is affected at each time by the instantaneous values of the tangential and normal components of the velocity along the entire boundary. In other words, the distribution of the vorticity in the whole domain is constrained by the velocity boundary values. A detailed description of the mathematical basis and the different numerical implementations of the orthogonal-projection operation of the vorticity field for the ($\boldsymbol{\omega}$, $\boldsymbol{\psi}$)

formulation can be found in.[1]

In our method, the issue of the vorticity boundary conditions on the no-slip surface is dealt with by a sequence of two solutions of the KLE under a different set of velocity boundary conditions. Thus, inside each time step, we perform two projectional operations of integral character applied on the velocity field which ensures that the vorticity evolves in time in a way compatible with the time-dependent velocity boundary values.

2 THE LAPLACIAN APPROACH AS A VORTICITY-VELOCITY METHOD THE KLE

Starting from the well-known vector identity:

$$\nabla^2 \boldsymbol{v} = \boldsymbol{\nabla} \cdot \boldsymbol{\nabla} \boldsymbol{v} = \boldsymbol{\nabla}(\boldsymbol{\nabla} \cdot \boldsymbol{v}) - \boldsymbol{\nabla} \times (\boldsymbol{\nabla} \times \boldsymbol{v}), \tag{1}$$

we found that a variational form of this "Laplacian" expression could be advantageously used as the spatial counterpart of the vorticity transport equation in a new type of vorticity-velocity method.

Let us consider the full three-dimensional incompressible Navier–Stokes equation in vorticity form for a flow domain Ω with solid boundary $\partial\Omega$ and *external* boundary of Ω in the far field, in a moving frame of reference fixed to the solid,

$$\frac{\partial \boldsymbol{\omega}}{\partial t} = -\boldsymbol{v} \cdot \boldsymbol{\nabla} \boldsymbol{\omega} + \nu \nabla^2 \boldsymbol{\omega} + \boldsymbol{\omega} \cdot \boldsymbol{\nabla} \boldsymbol{v}. \tag{2}$$

If we have the velocity field $\boldsymbol{v}$ in Ω at a certain instant of time, we can rewrite (2) as

$$\frac{\partial \boldsymbol{\omega}}{\partial t} = -\boldsymbol{v} \cdot \boldsymbol{\nabla}(\boldsymbol{\nabla} \times \boldsymbol{v}) + \nu \nabla^2 (\boldsymbol{\nabla} \times \boldsymbol{v}) + (\boldsymbol{\nabla} \times \boldsymbol{v}) \cdot \boldsymbol{\nabla} \boldsymbol{v}, \tag{3}$$

and solve for $\boldsymbol{\omega}$ at each point of the discretization of Ω by integration of (3) using an ODE solver.

Now, let us revisit (1) but this time impose a given distribution for the vorticity field the rate of expansion:

$$\nabla^2 \boldsymbol{v} = \boldsymbol{\nabla} \mathcal{D} - \boldsymbol{\nabla} \times \boldsymbol{\omega}, \tag{4}$$

$$\boldsymbol{\nabla} \cdot \boldsymbol{v} = \mathcal{D}, \tag{5}$$

$$\boldsymbol{\nabla} \times \boldsymbol{v} = \boldsymbol{\omega}. \tag{6}$$

Here $\boldsymbol{\omega}$ is the vorticity field in Ω given by (3) and $\mathcal{D}$ is the corresponding rate of expansion (i.e. the divergence field). The KLE is essentially defined as a solution of (4) in its weak form under the simultaneous constraints (5) and (6).

Let us consider the orthogonal decomposition of the velocity field in its irrotational non-solenoidal component $\boldsymbol{v}_{\mathcal{D}}$, its solenoidal non-irrotational component $\boldsymbol{v}_{\omega}$ and its irrotational and solenoidal (i.e. , harmonic) component $\boldsymbol{v}_h$. Under prescribed boundary conditions for the normal component of the velocity and given distributions for the vorticity $\boldsymbol{\omega}$ and the rate of expansion $\mathcal{D}$, this decomposition $\boldsymbol{v} = \boldsymbol{v}_{\mathcal{D}} + \boldsymbol{v}_{\omega} + \boldsymbol{v}_h$ is uniquely determined (see sec. 2.7 of[17]). Constraints (5) and (6) ensure that $\boldsymbol{v}_{\mathcal{D}}$ and $\boldsymbol{v}_{\omega}$ are properly solved.

$$\boldsymbol{\nabla} \cdot \boldsymbol{v} = \boldsymbol{\nabla} \cdot \boldsymbol{v}_{\mathcal{D}} = \mathcal{D}, \tag{7}$$

$$\boldsymbol{\nabla} \times \boldsymbol{v} = \boldsymbol{\nabla} \times \boldsymbol{v}_{\omega} = \boldsymbol{\omega}. \tag{8}$$

Now, applying the orthogonal decomposition to the total velocity field $\boldsymbol{v}$ in (4) we have,

$$\begin{aligned} \nabla^2(\boldsymbol{v}_h + \boldsymbol{v}_{\mathcal{D}} + \boldsymbol{v}_{\omega}) &= \nabla^2 \boldsymbol{v}_h + \boldsymbol{\nabla}(\boldsymbol{\nabla} \cdot \boldsymbol{v}_{\mathcal{D}}) - \boldsymbol{\nabla} \times (\boldsymbol{\nabla} \times \boldsymbol{v}_{\omega}) \\ &= \boldsymbol{\nabla}\mathcal{D} - \boldsymbol{\nabla} \times \boldsymbol{\omega}, \end{aligned} \tag{9}$$

substituting (7) and (8) in (9) it yields,

$$\nabla^2 \boldsymbol{v}_h = 0 \tag{10}$$

which provides the solution of the harmonic component $\boldsymbol{v}_h$. Thus, the KLE construction ensures that all three components of the velocity field are properly solved.

For incompressible cases, such as discussed here, $\mathcal{D}$ is simply set to zero. For compressible cases, $\mathcal{D}$ can be a general distribution given by a solution analogous to (3) but for the divergence transport equation (i.e. the momentum equation in divergence form) together with a solution of the mass transport equation and adding to (2) and (3) the terms eliminated by the application of the incompressibility condition.

Now, provided that we can find a way of imposing on the velocity field the no-normal-flow condition,

$$\boldsymbol{v} \cdot \boldsymbol{n} = 0, \tag{11}$$

and the no-slip condition,

$$\boldsymbol{v} \cdot \boldsymbol{\tau} = 0, \tag{12}$$

on the solid boundary $\partial\Omega$ in a way compatible with the vorticity distribution at that time, we obtain a compatible solution for the velocity. Then, from this velocity field we produce the right-hand side of (3) required to advance the time-integration process to the next step. In order to impose the no-normal-flow and no-slip conditions on $\partial\Omega$ together with the correspondingly compatible boundary conditions on the vorticity, we designed a scheme based on two consecutive solutions of the KLE, which goes as follows:

i. given a vorticity-compatible velocity field for the previous time-step $\boldsymbol{v}^{n-1}$, compute $\boldsymbol{\omega}^n$ by time integration of (3).

ii. get $\boldsymbol{\omega}_0^n$ by setting homogeneous conditions on $\partial\Omega$ for $\boldsymbol{\omega}^n$ (i.e. , set $\boldsymbol{\omega}^n$ to zero on $\partial\Omega$).

iii. compute a *free-slip* velocity field, $\tilde{\boldsymbol{v}}^n$, by solving (4)–(6), with $\mathcal{D} = 0$, for $\boldsymbol{\omega}_0^n$ applying only the no-normal-flow ($\boldsymbol{v} \cdot \boldsymbol{n} = 0$) condition on $\partial\Omega$.

iv. compute a new vorticity field, $\tilde{\boldsymbol{\omega}}^n$, from the curl of $\tilde{\boldsymbol{v}}^n$ with the no-slip condition on $\partial\Omega$ imposed, (thus obtaining a modified vorticity field in response to the induced slip).

v. compute the new vorticity-compatible velocity field, $\boldsymbol{v}^n$, by solving (4)–(6) using $\tilde{\boldsymbol{\omega}}^n$ and applying both the no-normal-flow and the no-slip condition on $\partial\Omega$.

In steps (iii)–(v) we apply the corresponding time-dependent, Dirichlet conditions for the velocity on $\partial\Omega_\infty$, the *external* boundary of Ω in the far field.

The algorithmic sequence defined in (i)–(v) has the advantage of producing a complete decoupling between the time integration of the vorticity transport equation and the space solution of the Poisson equation for the velocity field. The linear spatial solution defined in (4)–(6) (i.e. , the KLE) can be implemented in just one variational formulation. This implementation leads to a global matrix which is independent both of time and of the particular constitutive relation of the continuum media. Then, this matrix can be factorized at the moment of assembling and its triangular factors used as many times as needed so long as we are using the same grid. As we said, this is so even for problems with different constitutive relations because all the physics of the problem is taken into account only in the time-integration process for the vorticity, i.e. the spatial solution is purely *kinematic*. Thus, the space solution performed at each time step reduces to a pair of back-substitution processes where we simply change the right-hand side vector of the linear system in order to impose consecutively the boundary conditions (11)–(12). This scheme simplifies the issue of obtaining the vorticity in order to satisfy the boundary conditions on the velocity. Note that it is not a purely local manipulation performed on the boundary, this double solution of the velocity field is calculated over the entire domain involving two projectional operations of nonlocal character.

3 NUMERICAL IMPLEMENTATION OF THE KLE METHOD

For the discretization of the KLE in two-dimensional applications we used nine-node biquadratic isoparametric finite elements, which though "expensive" in computational terms possess a high convergence rate and, due their biquadratic interpolation of the geometric coordinates, provide the additional ability of reducing the so-called skin-error on curvilinear boundaries when compared to linear elements. Figure 1 shows the biquadratic interpolation functions (h^k, $k = 1, \ldots, 9$) of the nine-node isoparametric element on its natural system of coordinates (r,s) (for a detailed description of the isoparametric-element technique and its corresponding interpolation functions see[18]).

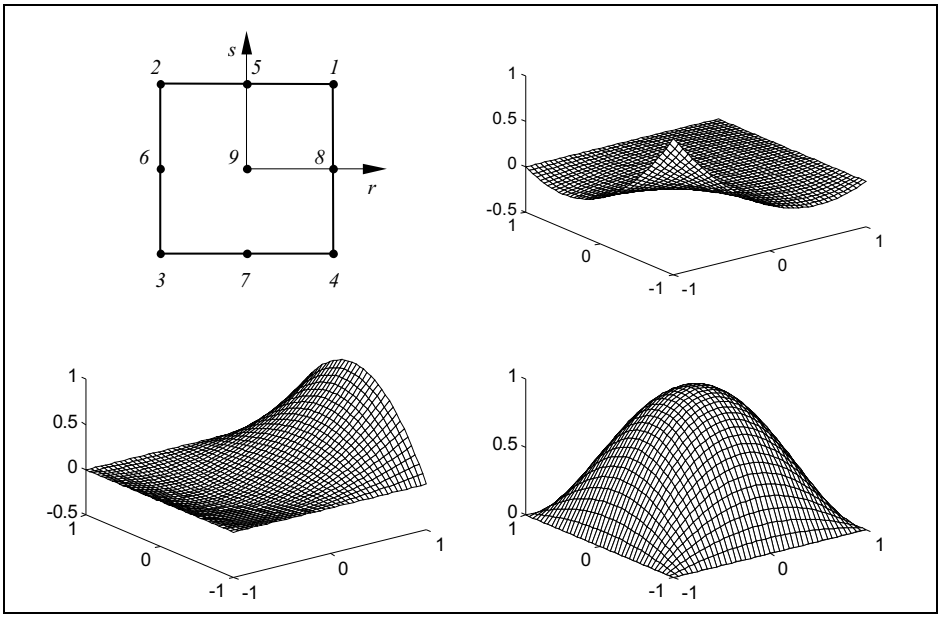

Figure 1: Interpolation functions of the nine-node isoparametric element showing its natural system of coordinates, node numeration and three examples of functions: for a corner node (node 3), for a central-lateral node (node 8) and for the central node (node 9).

In order to combine the power of convergence of the nine-node quadrilateral isoparametric element with the geometrical ability of a triangular grid to create suitable non-structured meshes with gradual and smooth changes of density, we implemented what we called tri-quadrilateral isoparametric elements.[19,20] The tri-quadrilateral elements consist of an assembling of three quadrilateral nine-node isoparametric elements in which each triangle of a standard unstructured mesh is divided into. Figure 2 shows a schematic example of a mesh of tri-quadrilateral finite elements obtained from the original triangular discretization.

Another advantage of the tri-quadrilateral scheme is that, by a previous condensation of the nodes that lie inside the triangle, we can significantly reduce the number of nodes to

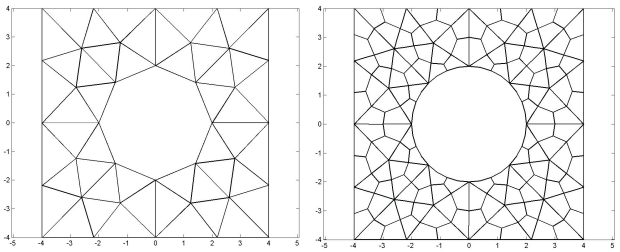

Figure 2: An example of a mesh of tri-quadrilateral finite elements obtained from a standard triangular discretization.

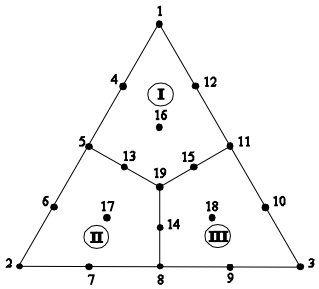

Figure 3: Schematic view of the internal topology of the tri-quadrilateral element. Subelements (I)–(III) are model by standard nine-node isoparametric interpolation. Numbers 1–19 indicate the in-triangle nodal numeration.

solve in the final system, subsequently recovering the values for the internal nodes from the solution on the non-condensable nodes. Figure 3 shows a schematic view of the internal topology of the tri-quadrilateral element including the in-triangle global numeration of the nodes and indicating the three nine-node subelements (I)–(III).

The internal nodes 13–19 may be expressed in terms of nodes 1–12 which lay on the elemental boundary following the classical procedure for elemental condensation (see[18]). This process of condensation allows us to reduce the size of the new system to solve to approximately a 40% of the original system. As it was mentioned above, none of the matrices involved in the finite element solution depend on $\boldsymbol{\omega}$ nor t, so they can be computed once for a given mesh, stored and used as many times as needed to compute the solution for the discrete velocity field $\hat{\boldsymbol{V}}$. The global matrix of the system is symmetric and positive definite, so it lends to factorization by Cholesky decomposition and its triangular factor is repeatedly used to solve $\hat{\boldsymbol{V}}$ through back-substitution.

For the implementation of the time-integration procedure we evaluate the right-hand side of (3) applying the corresponding differential operators onto the discrete velocity field $\hat{\boldsymbol{V}}$ calculated following steps (ii)–(v) in section (2). The normal procedure to calculate derivatives on the nodes of a mesh of isoparametric elements consists in computing the derivatives in the Gaussian points adjacent to each node and interpolate their results following several alternatives techniques. A detailed description of the this procedure can be found in.[18] In our case we used area-weighing interpolation which prove to be very effective. The contribution of each Gaussian point to its corresponding node depends on the constitution of the mesh and can be calculated at the moment of assembling. A set of arrays that perform the differential operations is assembled simultaneously with the finite-element matrices, so they can also be computed once for a given mesh, stored and used as many times as needed to provide evaluation of (3) right-hand side for an advanced package ODE solver. We choose a multivalue variable-order Adams-Bashforth-Moulton predictor-corrector (ABM-PECE) solver with adaptive stepsize control which proved to be quite efficient for this application. We also tried a fifth order adaptive-stepsize Runge-Kutta algorithm with good results. For the first DNS low-Reynolds-number applications

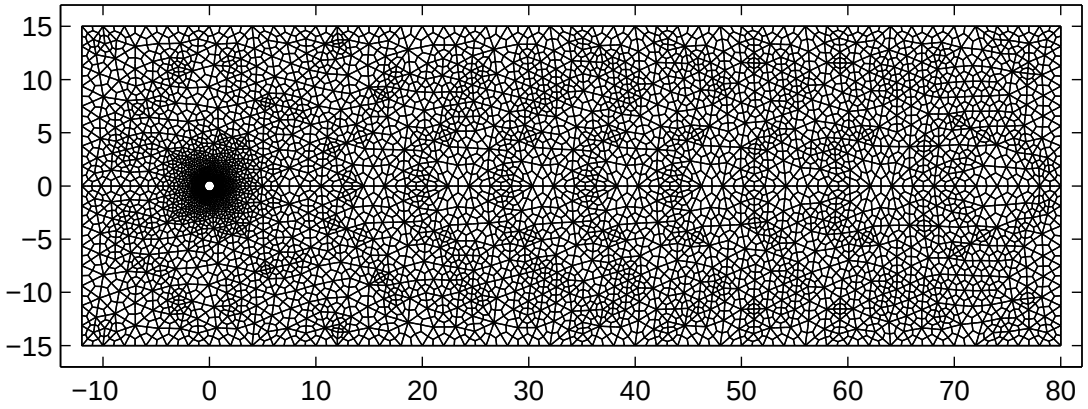

Figure 4: An example of a mesh of tri-quadrilateral finite elements used for the present analysis (geometrical coordinates are given in diameters).

of the KLE method, the function prove to be smooth enough for the adaptive ABM-PECE algorithm to work very efficiently, in these smooth cases the predictor-corrector outperforms other alternatives like the Bulirsch-Stoer method.[21]

4 SOME EXAMPLES OF APPLICATION OF KLE METHOD

We first show some results produced by the KLE method for the well-studied case of a circular cylinder started impulsively and then subjected to steady translational motion through fluid otherwise at rest. Figure 4 shows an example of a mesh of tri-quadrilateral elements used.

We shall see results at several values of Reynolds number, $Re = U\,d/\nu$, where U is the horizontal translational speed of the cylinder, d its diameter, and ν the kinematic viscosity of the fluid. We compare our two-dimensional flow simulations on the range $5 < Re < 180$ to experimental measurements and flow visualizations. Figure 5 shows velocity arrow-plots taken from our computations superimposed on two aluminum-dust flow-visualization plates due to S. Taneda (taken from[22]). In the range $5 < Re < 40$ we measured the length (s) of the stationary twin-vortex wake from the rear stagnation point on the solid surface to the confluence point at the tail of the wake, and we compared our results to the classical experiments of.[23] The results for the non-dimensional length s/d against Re are shown in figure 6. Overall the agreement between computations and experiments is very good.

As a second test case we considered the formation of the familiar Kármán vortex street behind a translating cylinder. Figure 7 shows a comparison between a smoke-in-air flow visualization due to M. M. Zdravkovich (taken from[22]) and the vorticity field produced by our numerical method at the same Reynolds number. We show a symmetric gray-scale map so areas of both positive and negative vorticity appear clear while zones of low

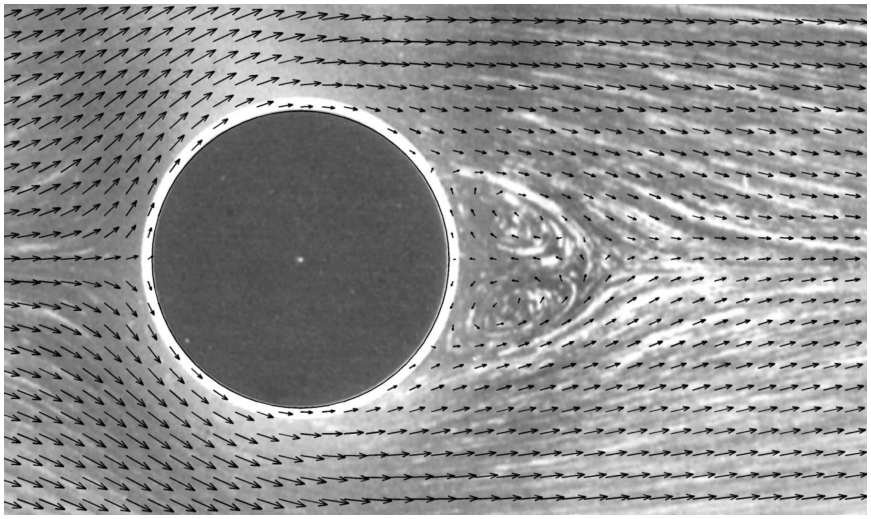

(a)

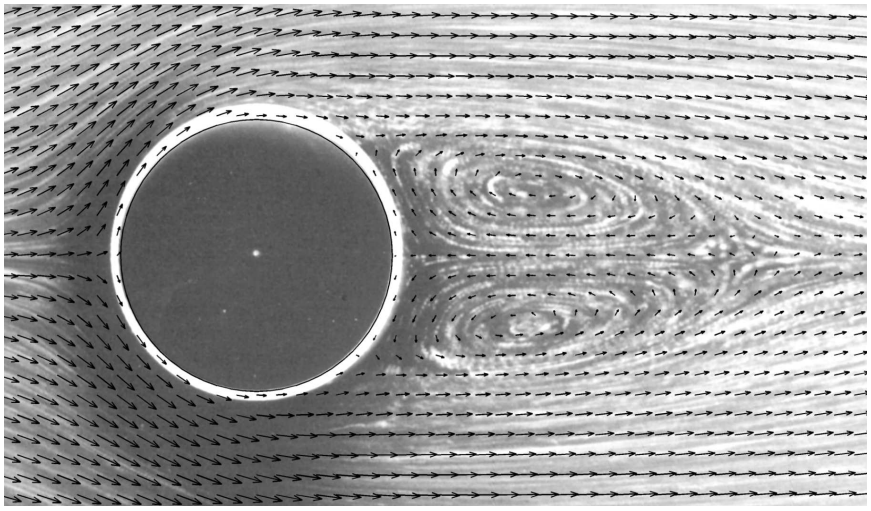

(b)

Figure 5: Comparison of flow visualizations by S. Taneda and arrow-plots from numerical results for the twin-vortex wake behind a cylinder at (a) $Re = 13.05$ and (b) $Re = 26$.

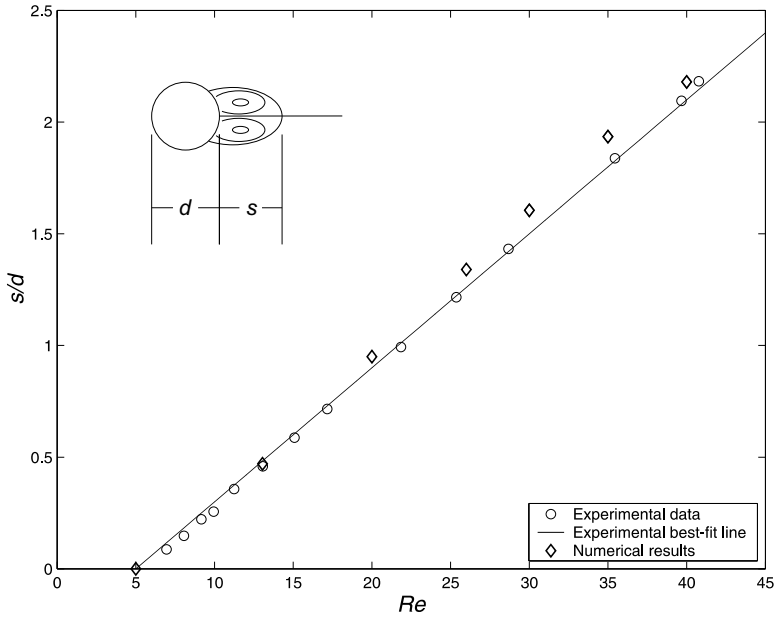

Figure 6: Comparison of the wake length calculated by the kinematic Laplacian equation method and the experimental measurements by S. Taneda.[23]

vorticity appear dark. The smoke 'signal' in the experimental photo, and the magnitude of vorticity displayed from the computation are, of course, not the same. Nevertheless, the correspondence in the spacing, and even the shape of the vortices, lends considerable confidence to the fidelity of the numerical simulations.

As our third test case, we measured the dominant frequency, f, of vorticity fluctuations at a set of points in the vortex street wake for the range of Reynolds numbers $50 < Re < 180$, and we computed the corresponding value of the Strouhal number ($St = fd/U$). The dominant frequency is the same for all the points probed, and it is clearly defined at an early stage of wake formation. The amplitude of the fluctuations, on the other hand, displays a transient state until it reaches its final, constant value somewhat downstream. Plotting St versus Re, as shown in figure 8, compares very favorably with the experiments presented by Williamson.[24]

Finally, we have recently started a study on the formation, shedding and further evolution of periodic vortex-array structures produced in the wake of forced-oscillating cylinders. Several qualitatively distinct wake regimes were observed experimentally depending on the wavelength of the undulatory motion of the cylinder and the amplitude of the transverse undulations. For instance, for a certain range in the combination of the wavelength/amplitude parameters, a pattern in which one pair and a single vortex are shed in each cycle of the forced oscillation is produced. This pattern is commonly know as P+S (one pair plus one single vortex). Figure 9 shows a comparison of a gray scale plot of the vorticity field calculated by the KLE method with an experimental laser-fluorescene

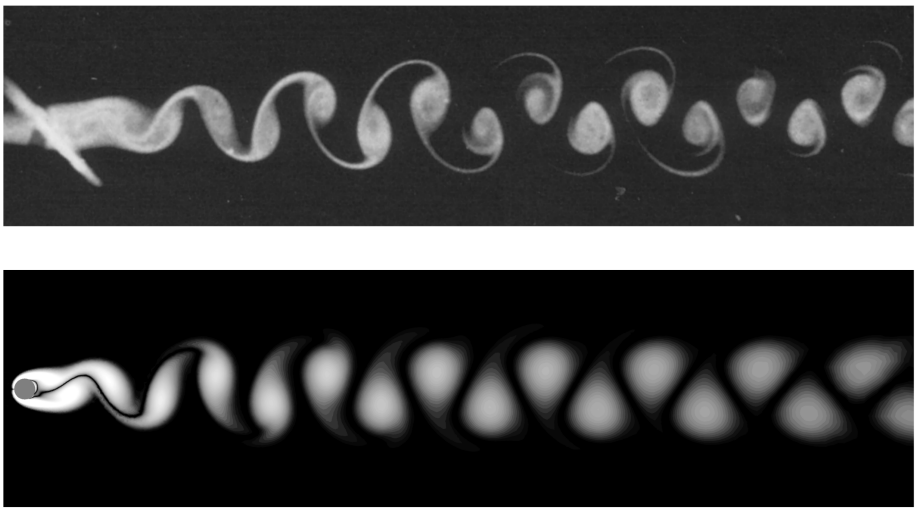

Figure 7: Comparison of flow visualization of a Kármán vortex street behind a cylinder at $Re = 100$ by M. M. Zdravkovich with a gray scale plot of the vorticity field produced by the kinematic Laplacian equation method at the same value of Reynolds number.

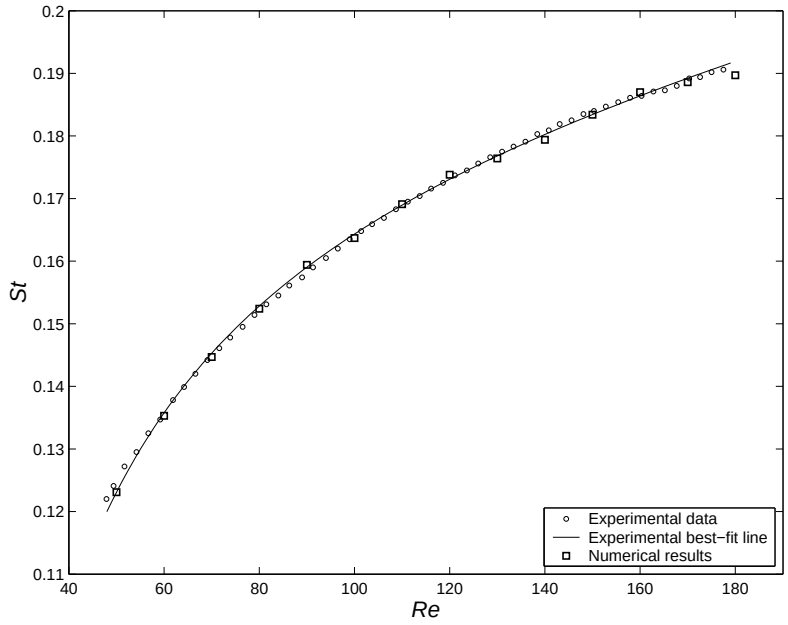

Figure 8: Comparison of the Strouhal number calculated by the kinematic Laplacian equation method and the experimental measurements by Williamson[24] for $Re < 180$.

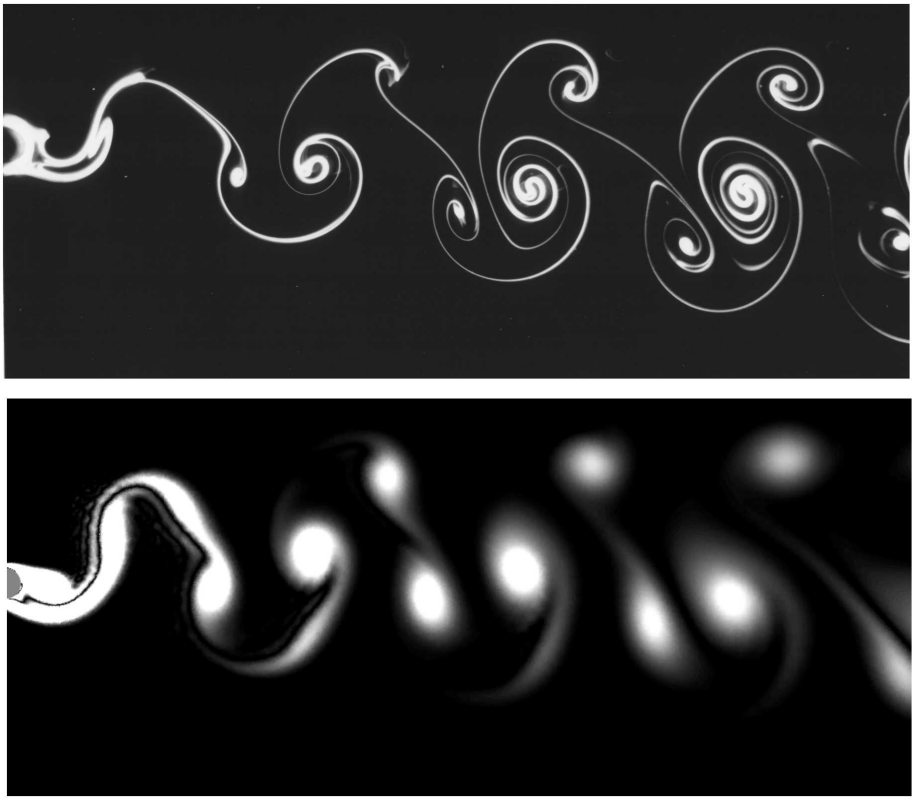

Figure 9: Comparison of flow visualization of a P+S wake of an oscillating cylinder for $Re = 140$ by C. H. K. Williamson (private communication to H. Aref) with a gray scale plot of the vorticity field produced by the KLE method at the same Reynolds number.

photograph for an oscillating cylinder at $Re = 140$. This photo was kindly provided by Prof. C. H. K. Williamson.

5 CONCLUSIONS AND OUTLOOK FOR FURTHER WORK

We have introduced a mathematical-computational approach to solve the time-dependent flow in a noninertial frame of reference attached to a body in translational and/or roto-translational motion. The KLE method was validated for two-dimensional DNS applications against experimental results for incompressible flow around circular cylinders at low Reynolds number, founding very good agreement.

As we have seen above, the basic formulation of the KLE is three-dimensional and has no special requirements on the rate-of-expansion distribution which is imposed. It implies that the method can be extended to the analysis of compressible flows, provided that we find a way of dealing with compatible boundary conditions for the rate-of-expansion in an analog way as we do with the vorticity.

Since it is a new approach, we are still exploring KLE method capabilities to man-

age higher Reynolds-number flows in DNS, and its potential to be extended to LES applications. The fact that the linear spatial solution provided by the KLE is purely kinematic with all the nonlinearities and the material constitutive properties remitted to the high-order adaptive time integration, favors the solution of problems with more complex constitutive relations like non-Newtonian, plastic or viscoplastic flows. And the same argument may be applied to the adoption of turbulence models for a future LES implementation of the method.

The KLE is based on a universal vectorial relation, so it can be used to solved any vector field provided that we can solve a transport equation for its divergence and curl. This together with the fact that time is the only iteration variable present, makes possible to extend its application to other physical problems like electromagnetic fields. It is also possible to couple the fluid analysis with other physical processes (e.g. , heat transfer or chemical reaction) by adding more equations to the ODE system, using grids with different densities for problems with different scales.

Regarding the numerical implementation of the KLE method, the techniques mentioned above: Cholesky decomposition/back-substitution for the spatial solution and adaptive predictor-corrector solver for time integration, prove to be very efficient for a two-dimensional low Reynolds number implementation of the method in a sequential code. In view to solve problems in complex geometries in three-dimensional applications which will require a substantial number of nodes (leading to large sparse systems) for the spatial discretization, it will be necessary to turn to a parallel version of the KLE code. This can be done in a relatively easy way: there are several parallel-program packages including parallel versions of the top ODE solvers and evaluation of our right-hand-side term involves matrix products that can be easily paralellizable. Concerning the solution of our linear system, back-substitution is essentially a sequential process, then it should be replaced by an iterative parallel linear solver. For a symmetric positive-definite matrix like ours, the preconditioned conjugate gradient method constitutes the first option, using the triangular factor from an incomplete Cholesky decomposition as preconditioner to accelerate convergence (like before, this incomplete Cholesky factor can be computed once an used repeatedly). Regarding the time integration process, the adaptive ABM-PECE solver works at its best for smooth functions, this situation could change when we try to extend the KLE method to problems with more complex constitutive relations or to the analysis of coupled physical processes where different time scales are likely too appear. If the function is no longer smooth, a recommendable alternative to the ABM-PECE solver is the adaptive Bulirsch-Stoer algorithm with modified midpoint integration and Richardson extrapolation.[21] If different time scales are present, the possibility of stiffness arises and then a Bulirsch-Stoer solver with semi-implicit midpoint integration is recommendable.

Finally, we may emphasize KLE flexibility to manage different trajectories with translational and rotational acceleration and its use of unstructured meshes. This method gives us a useful tool to study the vortex structure of wakes for different body shapes and

motions. We are using this tool to explore complex vortex wake patterns in the wake of forced oscillating cylinders at low Reynolds number, focusing on the process of splitting which characterizes the formation of P+S and similar structures. We hope to use the numerical tool developed here to continue with such explorations in the future.

6 ACKNOWLEDGMENTS

FLP is indebted to Hassan Aref for his advice, support and encouragement, and for many valuable discussions.

FLP is very grateful to the University of Buenos Aires for granting him a leave in order to complete this work. He would like to acknowledge the hospitality of the Department of Theoretical and Applied Mechanics at University of Illinois. This work was funded in part by research funds made available by University of Illinois.

REFERENCES

[1] L. Quartapelle, *Numerical solution of the incompressible Navier–Stokes equations*, Birkäuser, (1993).

[2] H. J. H. Clercx, "A spectral solver for the navier–stokes equations in the velocity-vorticity formulation for flows with two nonperiodic directions", *J. Comput. Phys.*, **137**, 186–211 (1997).

[3] C. G. Speziale, "On the advantages of the velocity-vorticity formulation of the equations of fluid dynamics", *J. Comput. Phys.*, **73**, 476–480 (1987).

[4] H. Fasel, "Investigation of the stability of boundary layers by a finite difference model of the Navier–Stokes equations", *J. Fluid Mech.*, **78**, 355–383 (1976).

[5] S. C. R. Dennis, D. B. Ingham, and R. N. Cook, "Finite difference methods for calculating steady incompressible flows in three dimensions", *J. Comput. Phys.*, **33**, 325–339 (1979).

[6] T. B. Gatski, C. E. Grosh, and M. E. Rose, "The numerical solution of the Navier–Stokes equations for 3-dimensional unsteady incompressible flows by compact schemes", *J. Comput. Phys.*, **82**, 298–329 (1989).

[7] M. Napolitano and G. Pascazio, "A numerical method for the vorticity-velocity Navier–Stokes equations in two and three dimensions", *Comput. Fluids*, **19**, 489–495 (1991).

[8] G. Guj and F. Stella, "A vorticity-velocity method for the numerical solution of 3D incompressible flows", *J. Comput. Phys.*, **106**, 286–298 (1993).

[9] G. Guevremont, W. G. Habashi, P. L. Kotiuga, and M. M. Hafez, "Finite element solution of the 3D compressible Navier–Stokes equations by a velocity-vorticity method", *J. Comput. Phys.*, **107**, 176–187 (1993).

[10] C. Davies and P. W. Carpenter, "A novel velocity-vorticity formulation of the Navier–Stokes equations with applications to boundary layer disturbance evolution", *J. Comput. Phys.*, **172**, 119–165 (2001).

[11] D. C. Lo and D. L. Young, "Arbitrary Lagrangian-Eulerian finite element analysis of free surface flow using a velocity-vorticity formulation", *J. Comput. Phys.*, **195**, 175–201 (2004).
[12] C. R. Anderson, "Observations on vorticity creation boundary conditions", In R. E. Caflisch, editor, *Mathematical Aspects of Vortex Dynamics*, pages 144–159. SIAM, (1988).
[13] A. J. Chorin, "Numerical study of slightly viscous flow", *J. Fluid Mech.*, **57**, 785–796 (1973).
[14] A. J. Chorin, "Vortex sheet approximation of boundary layers", *J. Comput. Phys.*, **27**, 428–442 (1978).
[15] L. Quartapelle and F. Valz-Gris, "Projections conditions on the vorticity in viscous incompressible flows", *Int. J. Numer. Meth. Fluids*, **1**, 129–144 (1981).
[16] L. Quartapelle, "Vorticity conditioning in the computation of two-dimensional viscous flows", *J. Comput. Phys.*, **40**, 453–477 (1981).
[17] G. K. Batchelor, *An introduction to fluid dynamics*, Cambridge University Press, (2000).
[18] K. J. Bathe, *Finite element Procedures*, Prentice Hall, (1996).
[19] F. L. Ponta and P. M. Jacovkis, "A vortex model for Darrieus turbine using finite element techniques", *Renewable Energy*, **24**, 1–18 (2001).
[20] F. L. Ponta and P. M. Jacovkis, "Constant-curl Laplacian equation: a new approach for the analysis of flows around bodies", *Comput. Fluids*, **32**, 975–994 (2003).
[21] W. H. Press, S. A. Teukolsky, W. T. Vetterling, and B. P. Flannery, *Numerical recipies in C, second edition*, Cambridge University Press, (2002).
[22] M. Van Dyke, *An album of fluid motion.* Parabolic Press, (1982).
[23] S. Taneda, "Experimental investigation of the wakes behind cylinders and plates at low Reynolds numbers", *J. Phys. Soc. of Japan*, **11**, 302–307 (1956).
[24] C. H. K. Williamson, "Oblique and parallel mode of vortex shedding in the wake of a circular cylinder at low Reynolds numbers", *J. Fluid Mech.*, **206**, 579–627 (1989).